AIAA AVIATION Forum
5-9 June 2017, Denver, Colorado
47th AIAA Thermophysics Conference

10.2514/6.2017-3487

Simulation of Oxygen Dissociation on a Six-dimensional O_4 Potential Energy Surface

Daniil A. Andrienko*

Iain D. Boyd †

Department of Aerospace Engineering, University of Michigan, Ann Arbor, MI, 48109

The quasi-classical trajectory method is applied to obtain the state-resolved dissociation rate coefficients of oxygen in collisions with another oxygen molecule. A six-dimensional potential energy surface, constructed using the double many-body expansion method is used. The results of simulation suggest that the O_2–O_2 rate coefficients can not be obtained by a scaling of a simpler O_2–O dataset, nor by applying the preferential dissociation model with a constant adjustable parameter. Depletion via an exchange mechanism significantly contributes to the total dissociation rate coefficient at temperatures below 5000K and at low vibrational energies. The new dataset of rate coefficients is used in a zero-dimensional heat bath simulation.

I. Introduction

The development and application state-resolved (SR) models of thermally nonequilibrium flows is a topic of increasing interest in aerothermochemistry. Resolving transitions between individual energy levels of species instead of assuming the Boltzmann population of these energy levels at some internal temperature is an important advantages of SR models over the conventional multi-temperature (MT) models. A large number of datasets aiming to fill the gap in state-specific RCs of air species was generated over the last decade due to ever-growing computational capabilities. Most of the studies are dedicated to three-body collisions, i.e. when a molecule (typically, either O_2 or N_2) collides with an atom. The SR simulation of molecule-molecule system is conducted less often due to either the absence of an adequate potential energy surface (PES) or due to the large cost of resolving all transitions between internal states arising in four-body collisions. Moreover, oxygen chemistry is studied less often compared to nitrogen, mainly because oxygen quickly dissociates during a flight of reentry vehicle. However, oxygen thermal relaxation and dissociation can be important for the design of hypersonic vehicles that travel at moderate hypersonic Mach numbers.

The SR simulation of oxygen shock flows is complicated by the presence of O_2–O_2 collisions that are dominant immediately behind the shock front due to the absence of atomic species. An accurate SR model would require a six-dimensional O_4 PES that accounts for the bond breaking mechanism. To the authors knowledge, a global *ab-initio* O_4 PES is yet to be proposed. The only O_4 PES that can adequately describe dissociation was developed by.[1] For this reason, the present paper concentrates on the O_2–O_2 state-resolved dissociative collisions using the Varandas PES.

The structure of the paper is as follows. Section II provides a discussion about the O_4 PES and four-body QCT simulations. Section III compares the QCT dissociation RC with the available theoretical and experimental data. Section IV presents the study of state-specific coefficients obtained in the O_4 QCT simulation. Conclusions are reported in Section VI.

II. O_4 potential energy surface and trajectory propagation

Previous studies of vibrational energy transfer in O_2–O_2 collisions were mostly concentrated on low temperatures that are of relevance for ozone formation in the upper atmosphere.[1–4] Billing and Coletti used

*Postdoctoral research fellow, Department of Aerospace Engineering, University of Michigan, 1320 Beal Ave
†James E. Knott Professor, Department of Aerospace Engineering, University of Michigan, 1320 Beal Ave

a semi-empirical PES that does not include bond breaking mechanisms. For this reason, the investigation in[4] is limited to temperatures up to 1000 K. In two former works, a six-dimensional double many-body expansion (DMBE I) PES is used, and is adopted in the present work. The DMBE I PES by Varandas is triplet and is designed to explain the "shadow" mechanism of ozone extinction:

$$\mathrm{O}\left({}^3P\right) + \mathrm{O}_3\left({}^1A_1\right) \rightarrow 2\mathrm{O}_2\left(X^3\Sigma_g^-\right) \tag{1}$$

Later, the DMBE I PES was revised by[5] in order to eliminate the spectator bond mechanism,[6] originally observed in trajectory simulations on the DMBE I PES. In the DMBE II PES, an extra four-body energy term of the extended Hartree-Fock type was added. This alleviates the probability of one oxygen molecules to emerge from the reaction with higher internal energy than the other O_2 molecule. However, as stated by,[5] this correction introduces a spurious minimum in the DMBE II PES which is yet to be eliminated. For this reason, the present work implements the original DMBE I PES.

The following reaction of state specific dissociation of oxygen is studied:

$$\mathrm{O}_2\left(v\right) + \mathrm{O}_2 \rightarrow 2\mathrm{O} + \mathrm{O}_2, \tag{2}$$

where the vibrational state of the first diatom is fixed while the vibrational state of the second diatom is sampled at some vibrational temperature T_v according to the Boltzmann distribution. Following this procedure, a SR dissociation rate coefficient (RC) of oxygen in vibrational state v is obtained. The quasi-classical trajectory (QCT) method is used to accumulate sufficient statistics of reaction (2). The details of the four-body QCT method are described elsewhere.[7]

The present in-house QCT code is capable of handling three- and four-body collisions (see[8] and references therein). For molecule-molecule simulations, the QCT code generates cross sections for nine possible channels: bound-bound inelastic channel, direct dissociation of target or projectile, double exchange of atoms, exchange with a subsequent dissociation of target or projectile, formation of a triatomic molecule, double dissociation and elastic collision. For the study of the SR target depletion, channels of direct dissociation and dissociation via exchange are important. The double dissociation channel contributes negligibly in the range of temperatures between 3000 and 15,000 K.

The DMBE I PES supports the formation of the triatomic molecule, i.e. ozone in a ground vibrational state. In the present work, O_3 formation is observed as well, however such trajectories are not counted toward the dissociation channel. In fact, capturing of such trajectories with short memory about initial state presents a computational challenge. The present study integrates trajectories for a sufficiently long time to ensure that formation of ozone is captured accurately.

The potential energy curve of diatomic oxygen generates 46 excited vibrational levels and a maximum of 234 rotational levels for the O_2 ground electronic state. The vibrational energies and turning points of each rovibrational state are calculated by the Wentzel-Kramers-Brillouin method. The total number of rovibrational levels in the ground electronic state of oxygen is 6,213, however, even numbered rotational states are not take into account to follow the selection rules of nuclear spin statistics. In all QCT calculations, the rotational states of both target and projectile are sampled according to the Boltzmann distribution at T_r=T, where T_r and T are the rotational and translational temperatures, respectively.

A database of bound-free RCs in the range of temperatures between 3000 and 15,000 K is generated. In theory, these rate coefficients should be modified to take into account two factors: A) the degeneracy of reactants and PES and B) the contribution of electronic states in the depletion mechanism. Ideally, these factors should be obtained from the trajectory branching via the QCT method that accommodates all possible PES that arise in O_2 (X)–O_2 (X) collisions and their intersections.[9] However, not only are such PESs unavailable, but also the branching in the QCT method would be prohibitively more expensive than the standard QCT method. Taking into account that the Varandas O_4 PES was derived using semi-empirical assumptions, the implementation of empirically derived corrections factors seems to be the most reasonable choice.

Since the O_4 PES describes the lowest energetic configuration of the O_3+O $\rightarrow 2O_2$ reaction, it is reasonable to assume that only 1/3 of reactions that lead to bound-bound transitions occur on this PES. Previously, a similar factor of 1/27 was applied for the O_2–O system when the QCT method was implemented on the $O_3(^1A_1)$ PES.[10] However, bound-free transitions can occur not only on the lowest PES. In fact, dissociation rate coefficients typically show a little sensitivity to PESs with different long range forces but with a similar short range repulsive wall. This was observed for O_2–N[11] and for O_2–O[12] collisions. Moreover, an *ab-initio* study of O_2-O_2 spin-spin interaction by[3] has revealed insignificant differences in a repulsive wall

between dimers in singlet, triplet and quintet states. Thus, the current approach assumes that dissociation RCs of reaction (2) on the DMBE I PES are similar to those on PESs of other degeneracy and, hence, no modification is needed, despite the fact that O_2–O_2 is 9-fold degenerate in the ground electronic state and the multiplicity of the DMBE I PES is only 3.

Meanwhile, the dissociation of molecular oxygen in shock waves with a temperature above a few thousands degrees is unlikely to proceed in an adiabatic manner. One way to account for alternative channels of dissociation from excited electronic states is to assume an equilibrium between lower vibrational levels of an excited electronic state and high vibrational levels of the ground state.[13] The contribution of dissociation from excited electronic states should be added to the dissociation RC from the ground electronic state. This assumption leads to the factor of 16/3, originally proposed by Nikitin for O_2 dissociation. This factor provides an excellent agreement between the QCT method and experimental data for O_2–O dissociation.[14] As will be shown later, the implementation of such a factor in O_2–O_2 dissociation RCs would lead to a strong overestimation of the experimental data. One of the reasons for this is due the fact that electronic excitation in O_2–O_2 collisions can be less efficient than in O_2–O collisions. This statement is based on intuition of strong attraction in the barrierless O_3 PES, when the projectile particle can closely approach the target, which results in the efficient "scrambling" of internal energy, and erases the memory of reactants about their initial state. The present O_4 PES is less reactive than the DMBE O_3 PES and, hence, the electronic excitation may not be that efficient. In fact, the global dissociation rate coefficient obtained via the DMBE I O_4 PES without additional modification for electronic excitation is closely described by the experimental RC.

Comparison of one-dimensional cuts of the O_4 PES is shown in Fig. 1 for the low intermolecular energies and in Fig. 2 for energies relevant to the present study. The long-range forces create attraction between two oxygen molecules. Both PESs developed by Aquilanti et al. and by Coletti and Billing are similar in the depth and the slope of the potential well. For some collisional configurations, such as X and H, the PES by Aquilanti is less attractive, and for other configurations the agreement between the Aquilanti and Coletti PESs is very good. The PES by Varandas is different from both other PESs for all considered collisional configurations. The former PES is less repulsive, and for X and H configurations the attractive part of the potential is non-monotonic.

The comparison of the repulsive part, shown in Fig. 2, is given only for the Varandas and Coletti PESs. In this case, large discrepancies are also observed. For all collisional configurations, Varandas PES is significantly more repulsive than the Coletti PES. These differences are an order of several eV at a fixed intermolecular distance. This is expected, since the Coletti PES includes only a pairwise exponential term given by short-range forces and does not include a four-body term, unlike the Varandas PES. The remaining differences between the considered PESs make an additional, possibly *ab-initio*, development of an O_4 potential highly desirable.

III. Results

A. Thermal equilibrium dissociation RC

One of the possible ways to validate the present dataset is to compare the QCT dissociation RC with the available experimental data. Usually, the thermally equilibrium RC, D^{EQ}, is reported in the literature, i.e. the dissociation rate that is observed when the population of the vibrational ladder corresponds to the Boltzmann distribution at given $T_v = T$. In order to obtain D^{EQ}, both vibrational states of reactants in Eq. (2) are sampled according to the Boltzmann distribution in the range of temperatures between 3000 and 15,000 K. For a realistic modeling of nonequilibrium flows, such a RC should be used together with a nonequilibrium dissociation model.

However, in shock tube measurements, a nonequilibrium dissociation RC, that corresponds to the non-Boltzmann population of the vibrational ladder, is actually measured. Often, this nonequilibrium dissociation RC is referred to as the quasi steady state (QSS) RC, D^{QSS}, since the most intense chemical transformations occur after the incubation period when the vibrational energy of the gas reaches a plateau. During the QSS phase, the gain of vibrational energy via the interaction of vibrational and translational modes is approximately equal to the loss of internal energy due to depletion. The effective dissociation RC is nearly constant, and it is smaller than D^{EQ} due to the underpopulation of excited vibrational states. This was demonstrated via the state-resolved simulations of N_2–N and O_2–O collisions using a high fidelity set of RCs.[14,15]

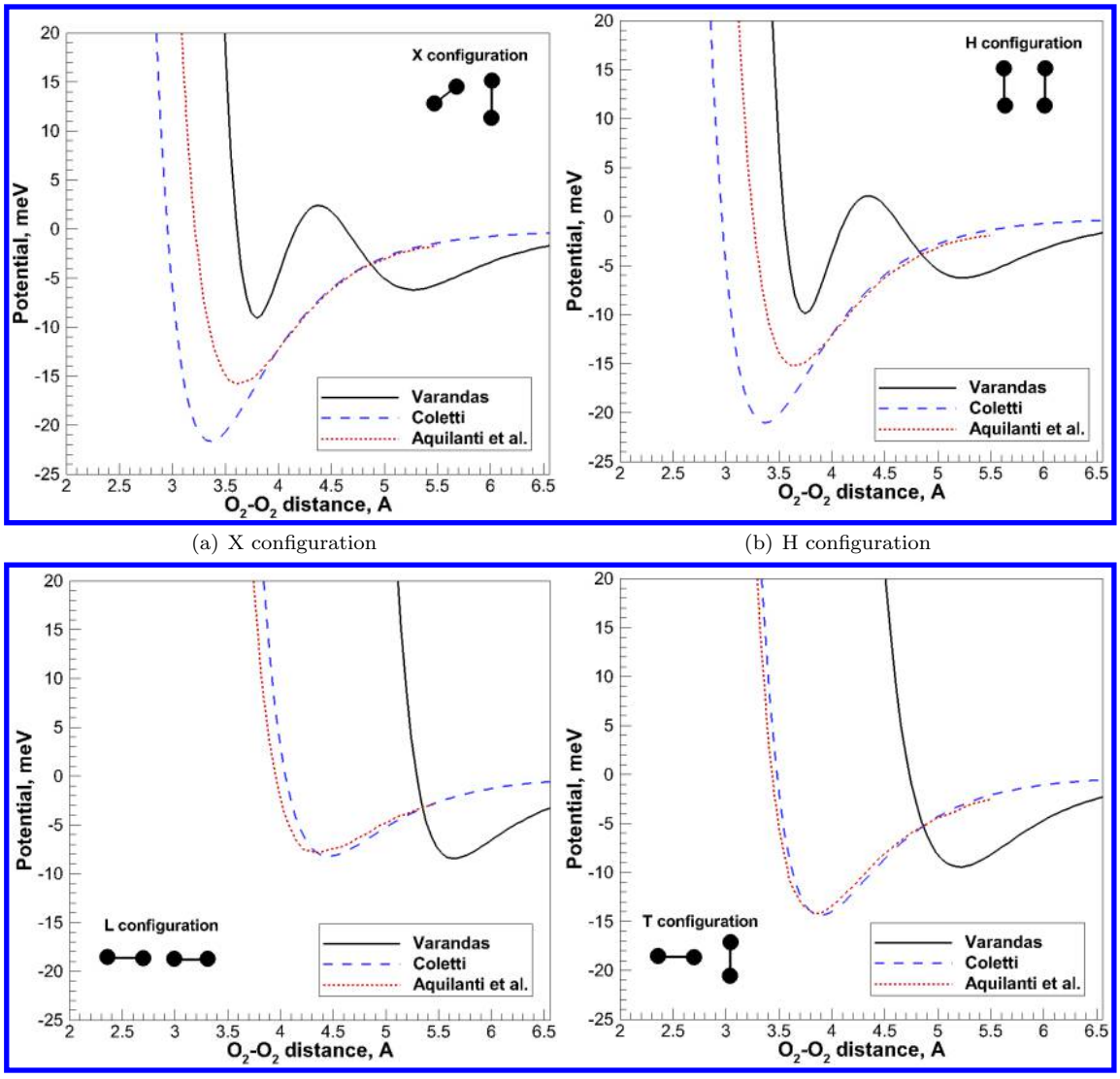

(a) X configuration

(b) H configuration

(c) L configuration

(d) T configuration

Fig. 1. Comparison of one-dimensional PES cuts using the data from Varandas et al.,[1] Aquilanti et al.[3] and Coletti et al.[4]

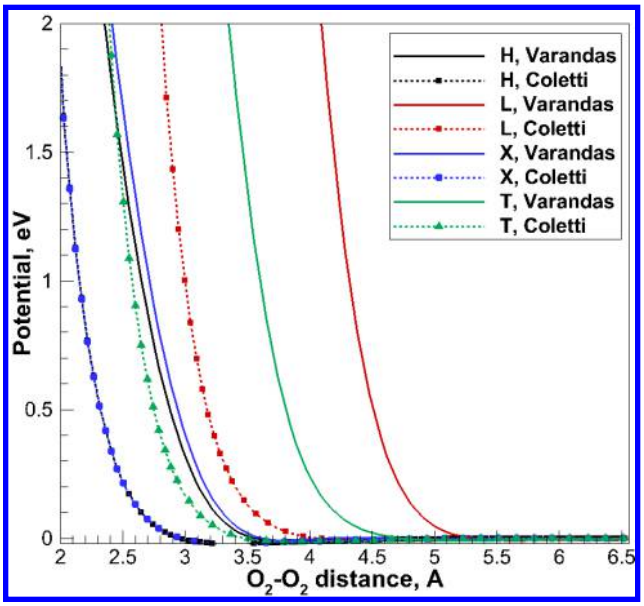

Fig. 2. Repulsive part of O_4 potential taken from Coletti et al.[4] and Varandas et al.[5]

It is possible to establish a relation between D^{EQ} and D^{QSS} using the Fokker-Planck equation for the diffusion component of the distribution function.[16] After some manipulations, the following expression is obtained:

$$D^{QS}(T,T_v) = D^{eq}(T,T_v)\,\frac{T}{T_v} exp\left(\frac{E_{D^*}}{k_B}\left(\frac{1}{T}-\frac{1}{T_v}\right)\right), \tag{3}$$

where E_{D^*} is the average loss of vibrational energy during dissociation: $E_{D^*} = E_D - \beta k_B T$, β is between 1 and 2. Some uncertainty in Eq. (3) is related to how the vibrational temperature T_v depends on T. In the experimental work by,[17] the dependence of T_v on T was derived using numerical solution of the two-temperature vibrational energy conservation equation along with the experimental measurements. In the present work, results shown by curve 1 in Fig. 2 in[17] are taken to model the dependence of T_v on T. Additionally, β is set to 2.

The present O_2–O_2 thermally equilibrium RC is shown in Fig. 3 by the solid line. For comparison, O_2–O D^{EQ}, obtained on a O_3 DMBE PES[14] is shown by the dashed line. The experimental data[17] is shown by empty circles. The equilibrium O_2–O_2 D^{EQ}, derived from shock tube measurements,[18] is shown by filled diamonds. Note, that the experimental data,[17] shown in Figs. 3 was processed using Eq. (3).

The QCT O_2–O_2 D^{EQ} agrees well with the experimental data for temperatures below 5000 K, and it is at the upper boundary of experimental data at T>5000 K. There is also very good agreement between the previously recommended RC[18] and the present data. As expected, dissociation in O_2–O collisions at the equilibrium population of the vibrational ladder at $T_v = T$ occurs nearly three times faster than in O_2–O_2 collisions.

The QCT dissociation RCs, shown in Fig. 3, were not modified for electronic excitation. In this case, good agreement is observed for temperatures below 7000 K. Being multiplied by a factor of 16/3, as was done for O_2–O, the present RC will strongly overestimate the experimental data. A possible explanation lies in the fact that the electronic excitation in O_2–O_2 collisions may be less efficient than in O_2–O, for which a factor of 16/3 was originally proposed. The effect of the additional four-body term, introduced in the MBE II PES, may contribute at these energies. Of course, there is also a possibility that the DMBE I PES is too reactive. In this case, an *ab-initio* study of the O_4 complex is highly desired.

In the future, when state-resolved bound-bound transition RCs become available, one can obtain the QS dissociation RC from master equation simulations, which allows a more direct comparison with the experimental data. From the experimental point of view, this can be attributed to the difficulties in measuring the QSS dissociation RC, since the QSS assumption may not be valid under strong thermal nonequilibrium. This and other factors lead to a large scatter in the experimental data, sometimes up to an order of magnitude. Nevertheless, satisfactory agreement between the QCT data and experimental measurements makes the state-resolved simulations of oxygen dissociation feasible. The present QCT data, shown in Fig. 3, can be curve fitted to the Arrhenius form:

$$D^{EQ} = 2.707\times10^{-3}T^{-1.319}exp\left(-6305/T\right),\ cm^3/s. \tag{4}$$

Using a set of state-specific dissociation RCs, it is possible to derive D^{QSS}, and perform a direct comparison with the experimental data and theoretical RCs recommended in the literature. A system of master equations, describing the population of individual vibrational states, is solved in a manner similar to O_2 relaxation in a heat bath of oxygen atoms.[14] For O_2–O_2 relaxation, a set of vibration-translation and vibration-vibration RCs is generated using the FHO model with the parameter of repulsiveness α=4.0 1/Å. Only O_2–O_2 collisions are considered, and O_2–O collisions are artificially excluded from simulations. A comparison of QSS RCs is shown in Fig. 4.

The QSS experimental data by Shatalov was calculated from the reported equilibrium values using Eq. (3). Diamond symbols correspond to the RC recommended in,[19] calculated at governing temperature $T_a = \sqrt{TT_v}$, where T_v corresponds to the vibrational temperature during the QSS phase. Solid and dashed lines describe O_2–O_2 and O_2–O QSS dissociation RCs obtained on O_4 and O_3 PESs.

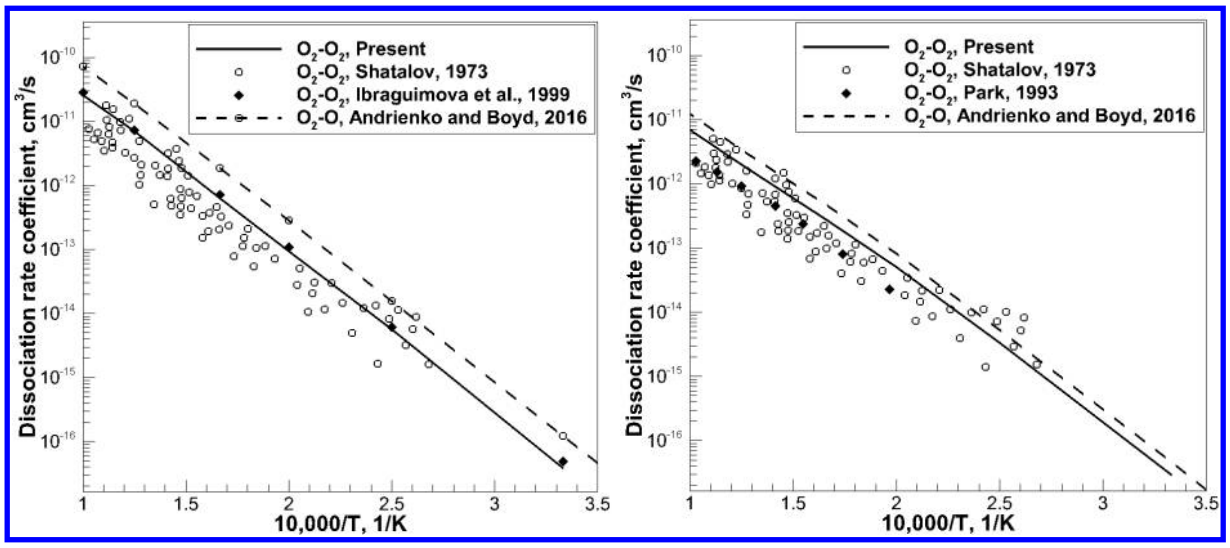

Fig. 3. Equilibrium dissociation RC of oxygen in O_2–O_2 and O_2–O collisions

Fig. 4. Quasi stationary dissociation RC of oxygen in O_2–O_2 and O_2–O collisions

The ratio of O_2–O_2 and O_2–O QSS RCs is smaller than the ratio of equilibrium RCs, shown in Fig. 3. At thermal equilibrium, the O_2–O RC is larger than the O_2–O_2 RC by a factor of 2.34 to 2.85. Under the QSS assumption, this ratio is only between 1.57 and 1.64. Overall, one can see that the present O_4 QCT data is at the upper boundary of the experimental dataset by Shatalov, while Park's O_2–O_2 RC is well within the measurements. An explanation of these discrepancies, based on state-specific analysis of the QSS RC, is given in the following section.

The present O_2–O_2 QSS dissociation RC obtained by solving a system of master equations using the QCT bound-free RCs and the FHO bound-bound RCs can be curve fitted to the Arrhenius form:

$$D^{QSS} = 3.717 \times 10^{-5} T^{-1.027} exp\left(-58540/T\right), \ cm^3/s. \tag{5}$$

IV. State-resolved $O_2(v)$–O_2 dissociation rate coefficients

Because the four-body QCT calculations are computationally expensive, the dissociation RCs are obtained only for v=0, 10, 20, 30 and 35 vibrational states and additionally for the last seven vibrational states v=40 ... 46. Missing RCs are obtained via an interpolation procedure.

The variation of the QCT RCs with vibrational energy is shown in Fig. 5. The state-specific dissociation RC is a semi-log function of vibrational energy for all but the very highest lying states. Namely, the semi-log dependence is only valid for energies less than 4.5 eV (v <35). At higher energies, the dissociation from the excited states occurs more rapidly. For this reason, the dissociation RCs for v = 40 ... 46 are obtained directly, rather than from the interpolation procedure.

In order to understand differences in the ratio of equilibrium and QSS dissociation RCs, the state-resolved QCT data is analyzed. Comparison of $O_2\,(v)$–O and $O_2\,(v)$–O_2 RCs, obtained on O_4 and O_3 PESs, is shown in Fig. 6 at temperatures of 3000 and 10,000 K. It follows immediately that $O_2\,(v)$–O_2 state-resolved RCs can be obtained at lower cost from $O_2\,(v)$–O by employing only a variable scaling factor, similarly to the approach in.[20] Recently, a similar scaling procedure was developed for N_2–N and N_2–N_2 collisions.[21]

At low temperatures, low-v bimolecular dissociation RCs are approximately twice larger than the $O_2(v)$-O dissociation RCs. Toward high vibrational states, O_2–O_2 dissociation RCs are smaller than the O_2–O RCs. At T=10,000K, $O_2(v)$–O_2 RCs are smaller than O_2–O RCs for all vibrational states. Note that the dissociation RC increases linearly in semi-log coordinates over a wide range of vibrational energy with the exception of highly-excited vibrational states. For these states, the increase of D_i occurs in a much faster

manner, compared to the rest of the ladder. This result is observed for both sets of QCT simulations on the O_4 and O_3 PESs.

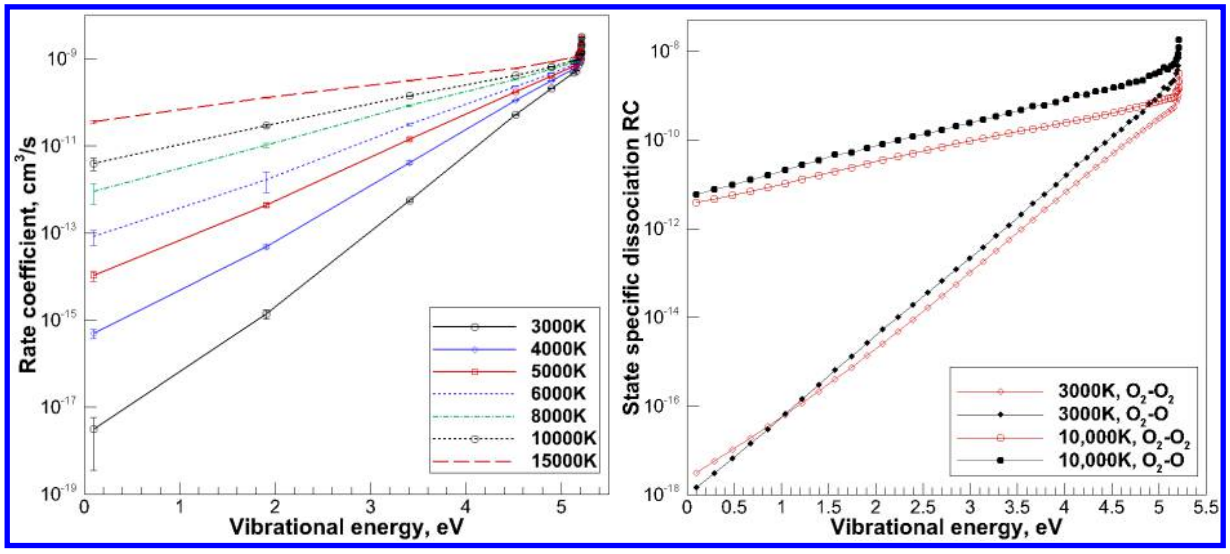

Fig. 5. Variation of the state-resolved dissociation RCs obtained on the O_4 PES with vibrational energy

Fig. 6. State-specific dissociation $O_2\,(v)$–O and $O_2\,(v)$–O_2 RCs at 3000 and 10,000 K

The contribution of specific states to the QSS dissociation RCs can be directly accessed from the master equation simulation. The cumulative contribution of individual vibrational states to D^{QSS} is shown in Fig. 7(a) for T=3000K and 10,000K and for O_2–O and O_2–O_2 collisions. For comparison, the contribution of individual vibrational states to the equilibrium dissociation RC is shown in Fig. 7(b).

At 3000 K, the cumulative curves for D^{QSS} are similar to those for D^{EQ}. This is explained by the small degree of nonequilibrium during the QSS state at mild heat bath conditions. Low vibrational states contribute to O_2–O_2 D^{QSS} noticeably more than to O_2–O D^{QSS}, particularly due to higher state-specific RCs and, at the same time, due to slower vibrational relaxation. The situation is different at 10,000 K. Due to strong nonequilibrium effects at this temperature, lower vibrational states contribute significantly more to D^{QSS} compared to their contribution at 3000K. This observation together with the discussion of Fig. 6 explains the smaller ratio of QSS RCs for O_2–O and O_2–O_2 collisions in comparison with the ratio of equilibrium dissociation RCs. In other words, the differences in ratio of dissociation RCs is due to high state-specific RCs generated on the O_4 Varandas PES as well as by a faster vibrational relaxation in the O_3 complex compared to that in O_4 at the studied temperatures.

It is interesting to compare the QCT state-specific O_2–O_2 RCs with those available in the literature. Besides the empirical model of preferential dissociation,[22] the FHO model[23] can be use to generate state-specific RCs of vibrational-vibrational, vibrational-translational energy transfer as well as of dissociation. The latter was performed da Silva[24] using the Morse potential with a repulsive parameter of 4.0 1/Å. The FHO model is a powerful tool and probably is one of the few alternatives to the QCT method when non-empirical RCs are desired. However, the FHO model does not take into account multiple channels of reaction that lead to thermodynamically indistinguishable products. In the case of O_4 simulations, it will be shown that both exchange and direct dissociation channels contribute significantly. At the same time, the effect of anharmonicity on the species composition can be significant as well, especially taking into account nonlinear increase of RCs for high-v states, shown in Fig. 5. The comparison of the FHO RCs with the present QCT dataset is given in Fig. 8(a) and 8(b) for low and high lying vibrational states. The contribution of exchange channel in the present QCT results is shown in Fig. 9.

For states with low vibrational energy, the QCT model provides RCs that are approximately 5 to 10 times higher than the FHO RCs. As vibrational energy increases, the differences between QCT and FHO models become small. The RCs for the last five vibrational states are plotted separately to emphasize the different temperature dependence of RCs. For the state located near the dissociation limit, the dissociation RC varies much slower than for states with low energy.

It follows that the exchange channel, when one of the atoms in a target molecule is replaced by an atom from the projectile diatom, and a newly formed target diatom dissociates, significantly affects properties

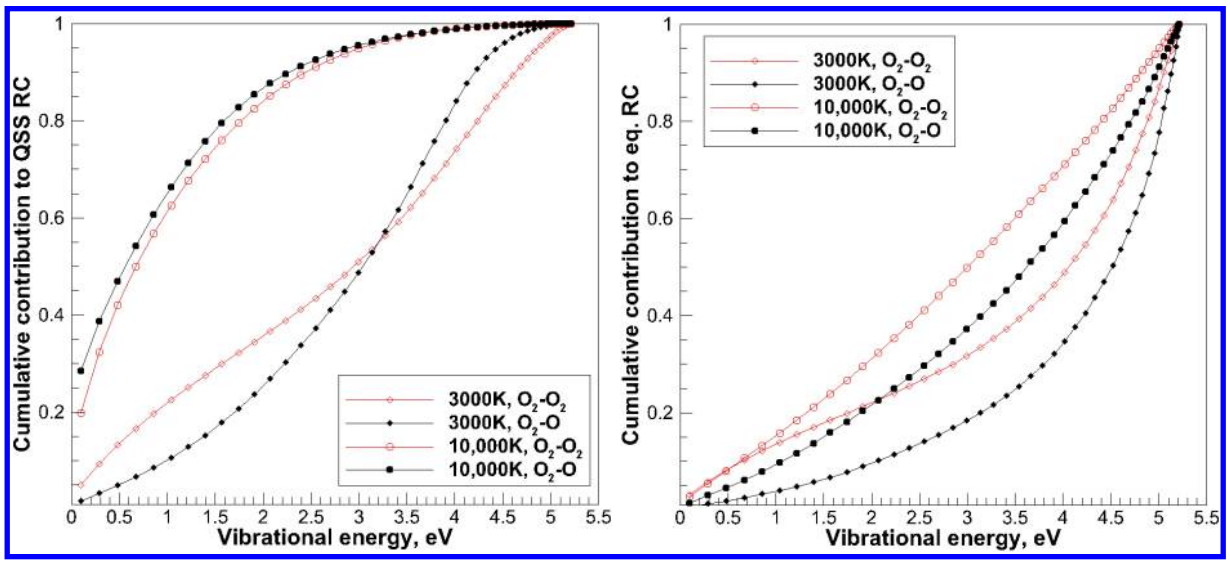

(a) QSS dissociation RC (b) Equilibrium dissociation RC

Fig. 7. State-resolved contribution of vibrational levels to dissociation RC at 3000 and 10,000 K

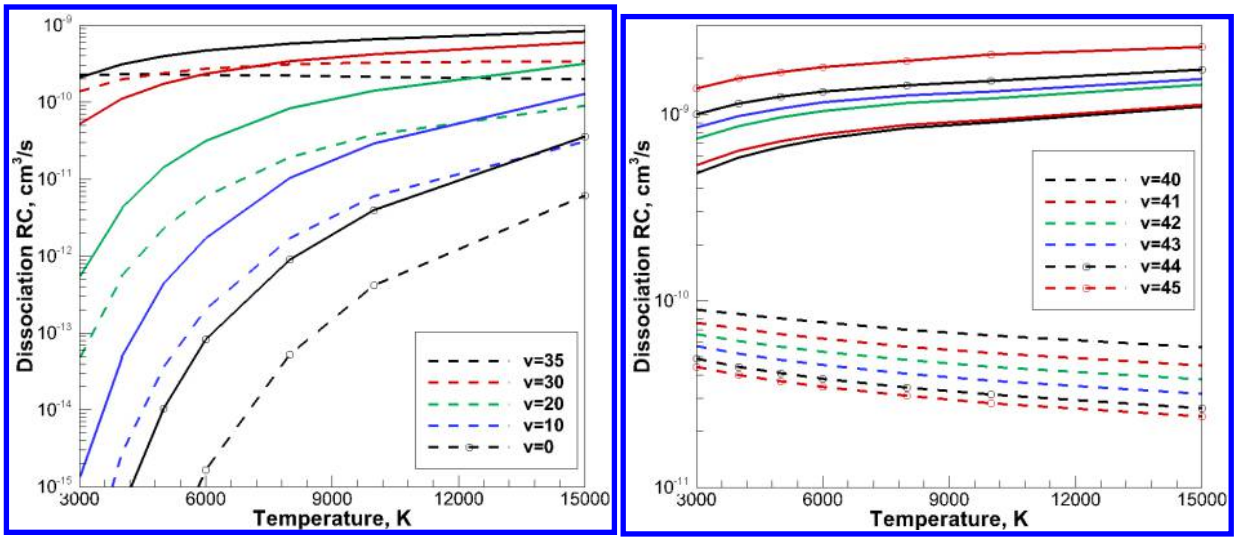

(a) Low vibrational states (b) Excited vibrational states

Fig. 8. Comparison of QCT and FHO[24] O_2–O_2 dissociation rate coefficients

of states with low vibrational energy in the entire range of studied temperatures. When both direct and exchange channels are taken into account, the QCT RC for v=0 is higher than the FHO RC by one to two orders of magnitude in the range between 3000 and 15,000 K. The QCT RCs, given by only the direct channel, show a better agreement with the FHO RCs compared to the total channel of reaction (2). The disagreement between the FHO and QCT models becomes smaller with the vibrational quantum number; and this can be partially attributed to the closure of the exchange channel.

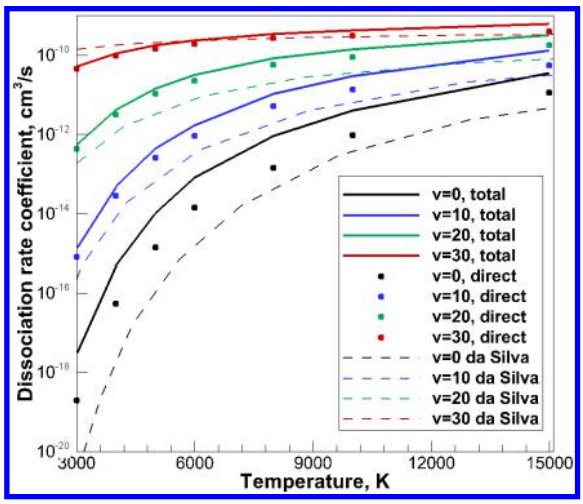

Fig. 9. FHO[24] and present QCT state-specific O2-O2 dissociation RCs

V. Heating and cooling heat bath conditions

The newly generated state-specific rate coefficients are applied to the simulation of vibrationally cold and hot oxygen in a heat bath with a constant translational temperature. In these simulations, both O_2–O and O_2–O_2 collisions are included. The O_2–O vibrationally resolved bound-free and bound-bound RCs were obtained previously[14] using the Varandas O_3 PES.[25] This PES can be obtained from the present O_4 PES by removing one of the atoms. The rotational structure of the rate coefficients, reported in Ref,[14] is averaged at a given translational temperature according to the Boltzmann distribution. For the O_2–O_2 bound-bound VT and VV rate coefficients, the FHO model[23] is used with a repulsive parameter of 4 Å^{-1}. Two sets of O_2–O_2 bound-free transitions are used. The first one is obtained via the O_4 QCT simulations. The second set is obtained by the FHO model with parameters described in Ref.[24] In other words, the simulation of the heat bath conditions is conducted with the O_2–O_2 dissociation dataset being the only varying parameter in a kinetic scheme.

First, a case of vibrationally cold gas is considered. The time evolution of vibrational temperature in a heat bath of 6000, 8000 and 10,000K and $T_v^0 = 100$K is shown in Fig. 10. Solid lines correspond to the solution obtained using the QCT dataset, the dashed lines describe the results of the FHO model. Initially, the flow contains only molecular oxygen with the number density of 10^{18} cm^{-3}. As follows from Fig. 8, at these translational temperatures the state-specific dissociation RCs, generated by the QCT model, are larger than those of the FHO model. Depletion of the O_2 vibrational ladder occurs more slowly when the FHO dataset is implemented, causing an increased vibrational temperature during the QSS phase, as can be seen in Fig. 10. Depletion of the vibrational ladder leads to the decrease of temperature during the QSS phase. The non-monotonic behavior of temperature is more pronounced at higher translational temperatures when the flow contains a significant amount of atomic oxygen, since the dissociation in O_2–O collisions is more effective than in O_2–O_2 collisions.

In strong shock flows, the influence of O_2–O_2 dissociative collisions is clearly important at the initial stage of the QSS phase being an initial source of atomic species. In a cooling gas at moderate initial vibrational temperatures, the influence of molecule-molecule collisions can be even more pronounced, since the fraction of molecular species remains large through out the entire process of relaxation. The present paper simulates a cooling flow with the following parameters: T=1000K, $T_v^0 = 2000$K and T=2000K, $T_v^0 = 3000$K. The initial fraction of atomic oxygen is set to the equilibrium value at $T = T_v^0$: at T=1000K, it is equal to 2.1×10^{15} cm^{-3}, t T=2000K it is set to 2.7×10^{17} cm^{-3}.

The QCT simulations of the state-specific dissociation RCs at low translational temperatures is a computational challenge. However, as follows from Fig. 5, there is a linear temperature dependence between the natural logarithm of a RC and the vibrational energy of a state, if the vibrational energy of this state is significantly below the dissociation limit. At the same time, the QCT simulation of excited vibrational states is less challenging when resolving the dissociation channel. For the present purposes, the QCT dissociation

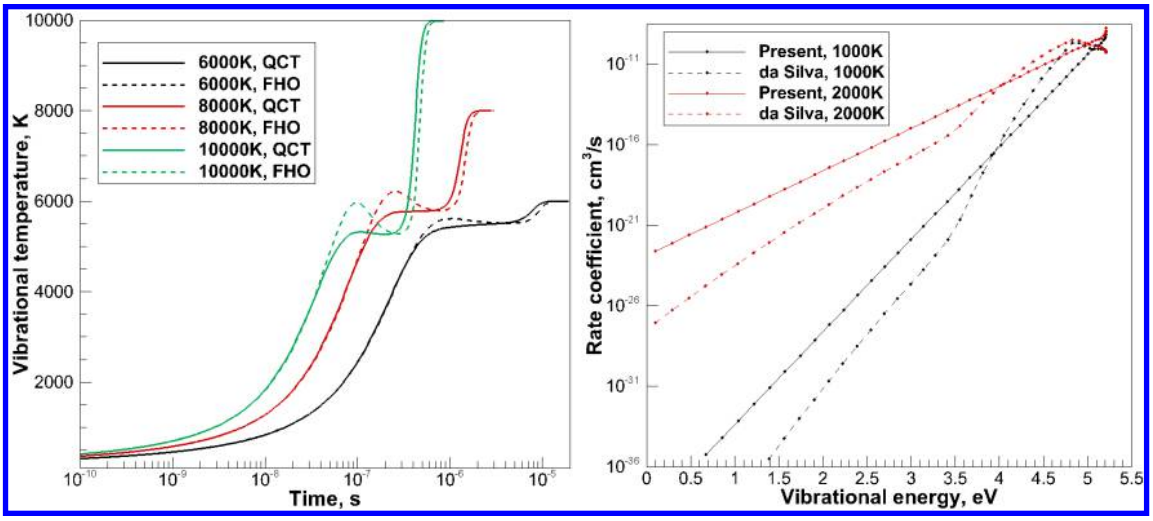

Fig. 10. Vibrational temperature at the heating bath conditions, T=6000, 8000, and 10000K, initial T_v=100K

Fig. 11. State-specific O_2–O_2 dissociation RCs at T=1000 and 2000K given by the FHO[24] and the present QCT models

RCs are obtained for selected states with $v \geq 20$ and the RCs of states with $v < 20$ are linearly extrapolated as described previously. The QCT and FHO O_2–O_2 dissociation RCs at T=1000 and 2000K are shown in Fig. 11 with the solid and dashed lines, respectively. The temperature dependence of the QCT RCs is similar to that at higher temperatures in Fig. 5. The FHO RCs for states with $e_v < 3.5$ eV are significantly smaller than the QCT RCs. The states with higher energy have a non-monotonic behavior for the FHO RCs, which can probably be considered as a deficiency of the FHO model.

The population of the vibrational ladder during thermalization is shown in Figs. 12 and 13 for the heat baths of 1000K and 2000K, respectively. Due to the low translational temperature, a preferential recombination to excited vibrational states takes place. The bound-bound energy exchange between these states is efficient due to the small spacing between vibrational levels. This explains the existence of the long-lived plateau. Due to the non-monotonic behavior of the O_2–O_2 FHO RCs, the population of states with $e_v \approx 4.5$ eV is significantly higher than that predicted by the QCT model. As the result, the plateau in the case of FHO model is densely populated, compared to the results of the QCT model. Differences between the QCT and FHO models for the heat bath with T=2000K are smaller, particularly because of the initial higher abundance of atomic oxygen at T_v^0= 3000K.

The influence of the O_2–O_2 dissociation model on macroscopic parameters, such as the species number density, is shown in Fig. 14. The QCT model predicts much faster recombination in the mixture with low translational temperature, compared to the FHO model. The differences in the composition of mixture with the higher initial fraction of atomic oxygen are smaller, as expected. Because at simulated conditions the plateau does not perturb the population of the lowest vibrational states, the vibrational temperatures given by the FHO and QCT models in all cooling heat bath conditions are similar to each other. This example demonstrates that the chemical composition in gas flows with $T_v > T$ is defined not only by the vibrational temperature but also depends on the kinetics of the excited vibrational states.

VI. Conclusion

A set of state-specific dissociation rate coefficients for molecular oxygen is generated. For the first time in the literature, the $O_2(v)$–O_2 dissociation RCs are obtained via the QCT method on a six-dimensional O_4 PES. Heat bath conditions are simulated using a system of master equations coupled to the new set of rate coefficients. Thermal equilibrium and QSS O_2–O_2 dissociation RCs are in satisfactory agreement with shock tube data, slightly overestimating the median experimental value at temperatures between 4000 and 10,000 K. The present set of dissociation RCs shows significant differences from those RCs obtained either via the preferential dissociation model or by means of the FHO model. This indicates the necessity in the QCT calculations on a more accurate O_4 PES in future.

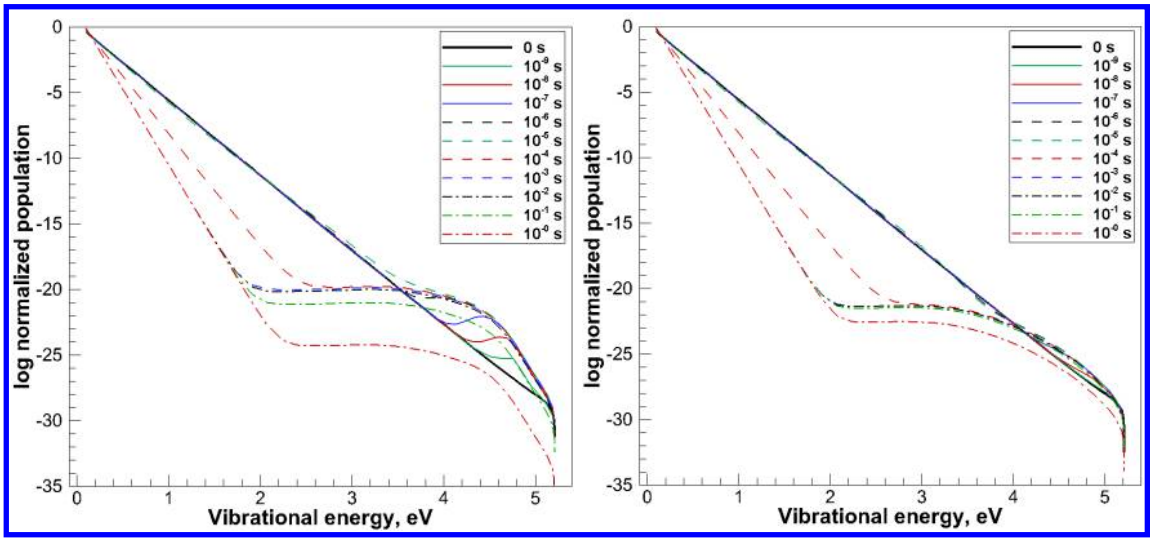

(a) FHO model (b) QCT model

Fig. 12. Population of vibrational ladder in the cooling heat bath conditions: T=1000K, initial T_v=2000K

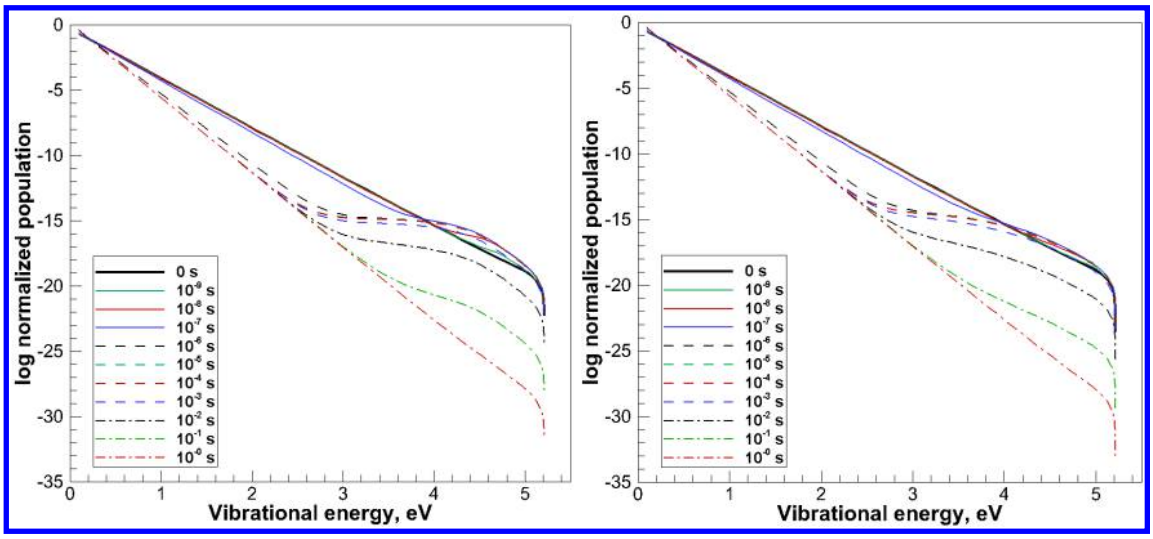

(a) FHO model (b) QCT model

Fig. 13. Population of vibrational ladder at the cooling heat bath conditions: T=2000K, initial T_v=3000K

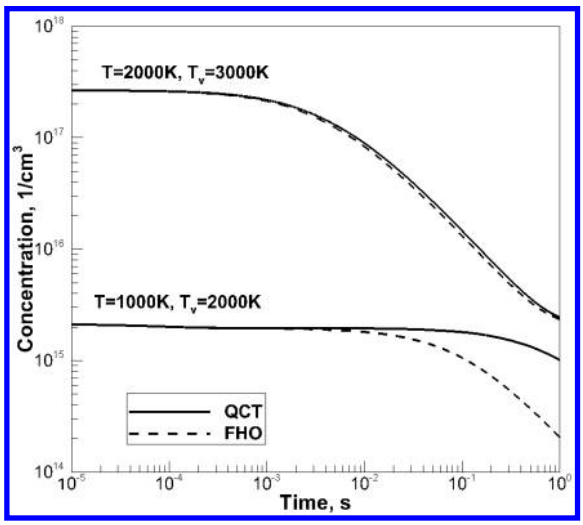

Fig. 14. Atomic oxygen number density in the cooling heat bath

Trajectory simulations, described in the present paper, revealed several interesting findings about the dissociation mechanism in O_2–O_2 collisions. First, the exchange channel contributes significantly to state-specific RCs, particularly at low temperatures and for states with low vibrational energy. Second, the state-specific O_2–O_2 dissociation RCs can not be obtained from O_2–O RCs using a constant scaling factor. In fact, RCs for low vibrational states are similar for O_4 and O_3 molecular systems, while the high-v states dissociate much faster in O_2–O collisions. These results should be viewed keeping in mind the accuracy of the DMBE method that was used to construct the O_3 and O_4 PESs.

Vibrational temperature during the QSS phase is sensitive to the O_2–O_2 state-resolved dissociation RCs. An implementation of the FHO and QCT models for a simulation of heat bath conditions indicates that the variation in vibrational temperature can be non-monotonic during the QSS phase if the energy removal in molecule-molecule collisions is slow. In a situation of a vibrationally hot gas in a cold heat bath, the formation of a long-lived plateau due to preferential recombination is observed. This process is also highly sensitive to the O_2–O_2 dissociation model.

VII. Acknowledgments

The authors gratefully acknowledge funding for this work through Air Force Office of Scientific Research Grant FA9550-16-1-0291. DA would like to thank Prof. António Varandas for the computer program of the O_4 PES.

References

[1]A. Varandas and A. Pais, "Double many-body expansion potential energy surface for O_4 (^{3}A), dynamics of the O (^{3}P)+ O_3 ($^1A_1$) reaction, and second virial coefficients of molecular oxygen," in *Theoretical and Computational Models for Organic Chemistry*, pp. 55–78, Springer, 1991.

[2]N. Balakrishnan, A. Dalgarno, and G. D. Billing, "Multiquantum vibrational transitions in O_2 ($v \geq 25$)+ o$_2$ (v=0) collisions," *Chemical Physics Letters*, vol. 288, no. 5, pp. 657–662, 1998.

[3]V. Aquilanti, D. Ascenzi, M. Bartolomei, D. Cappelletti, S. Cavalli, M. de Castro Vitores, and F. Pirani, "Molecular beam scattering of aligned oxygen molecules. the nature of the bond in the o2- o2 dimer," *Journal of the American Chemical Society*, vol. 121, no. 46, pp. 10794–10802, 1999.

[4]C. Coletti and G. D. Billing, "Vibrational energy transfer in molecular oxygen collisions," *Chemical physics letters*, vol. 356, no. 1, pp. 14–22, 2002.

[5]A. Varandas and J. Llanio-Trujillo, "Dynamics of O+ O_3 reaction on a new potential energy surface for ground-triplet tetraoxygen: Spectator bond mechanism revisited," *Journal of Theoretical and Computational Chemistry*, vol. 1, no. 01, pp. 31–43, 2002.

[6]J. Mack, Y. Huang, A. Wodtke, and G. C. Schatz, "The product vibrational, rotational, and translational energy distribution for the reaction O(^3P_j)+$O_3 \rightarrow 2O_2$: Breakdown of the spectator bond mechanism," *Journal of Chemical Physics*, vol. 105, no. 17, pp. 7495–7503, 1996.

[7]L. M. Raff, D. L. Thompson, L. Sims, and R. N. Porter, "Dynamics of the molecular and atomic mechanisms for the hydrogen-iodine exchange reaction," *Journal of Chemical Physics*, vol. 56, no. 12, pp. 5998–6027, 1972.

[8]D. Andrienko and I. D. Boyd, "State-resolved O_2–N_2 kinetic model at hypersonic temperatures," in *55th AIAA Aerospace Sciences Meeting*, p. 0659, 2017.

[9]D. G. Truhlar and J. T. Muckerman, "Reactive scattering cross sections iii: quasiclassical and semiclassical methods," in *Atom-Molecule Collision Theory*, pp. 505–566, Springer, 1979.

[10]A. Gross and G. D. Billing, "Isotope effects on the rate constants for the processes $O_2 + O \rightarrow O + O_2$ and $O_2 + O + Ar \rightarrow O_3 + Ar$ on a modified ground-state potential energy surface for ozone," *Chemical Physics*, vol. 217, pp. 1–18, 1997.

[11]D. A. Andrienko and I. D. Boyd, "Thermal relaxation of molecular oxygen in collisions with nitrogen atoms," *Journal of Chemical Physics*, vol. 145, no. 1, p. 014309, 2016.

[12]D. Andrienko and I. D. Boyd, "Investigation of oxygen vibrational relaxation by quasi-classical trajectory method," *Chemical Physics*, vol. 459, pp. 1–13, 2015.

[13]E. Nikitin, *Theory of elementary atomic and molecular processes in gases*. Oxford, Clarendon Press, 1974.

[14]D. A. Andrienko and I. D. Boyd, "Rovibrational energy transfer and dissociation in O_2–O collisions," *Journal of Chemical Physics*, vol. 144, no. 10, p. 104301, 2016.

[15]M. Panesi, R. L. Jaffe, D. W. Schwenke, and T. E. Magin, "Rovibrational internal energy transfer and dissociation of $N_2(^1\Sigma_g^+)$- $N(^4S_u)$ system in hypersonic flows," *Journal of Chemical Physics*, vol. 138, no. 4, p. 044312, 2013.

[16]S. A. Losev and V. A. Polyanskii, "Effect of vibrational relaxation of molecules on dissociating air characteristics behind a strong shock front," *Fluid Dynamics*, vol. 4, no. 4, pp. 84–90, 1969.

[17]O. Shatalov, "Molecular dissociation of oxygen in the absence of vibrational equilibrium," *Combustion, Explosion, and Shock Waves*, vol. 9, no. 5, pp. 610–613, 1973.

[18]L. Ibragimova, G. Smekhov, and O. Shatalov, "Dissociation rate constants of diatomic molecules under thermal equilibrium conditions," *Fluid Dynamics*, vol. 34, no. 1, pp. 153–157, 1999.

[19]C. Park, *Nonequilibrium hypersonic aerothermodynamics*. Wiley, 1989.

[20]O. Kunova, E. Kustova, and A. Savelev, "Generalized treanor–marrone model for state-specific dissociation rate coefficients," *Chemical Physics Letters*, vol. 659, pp. 80–87, 2016.

[21]F. Esposito, E. Garcia, and A. Laganà, "Comparisons and scaling rules between (n)+N_2 and N_2+ N_2 collision induced dissociation cross sections from atomistic studies," *Plasma Sources Science and Technology*, vol. 26, no. 4, p. 045005, 2017.

[22]P. V. Marrone and C. E. Treanor, "Chemical relaxation with preferential dissociation from excited vibrational levels," *Physics of Fluids*, vol. 6, no. 9, pp. 1215–1221, 1963.

[23]I. V. Adamovich, S. O. Macheret, J. W. Rich, and C. E. Treanor, "Vibrational relaxation and dissociation behind shock waves. part 1-kinetic rate models.," *AIAA Journal*, vol. 33, no. 6, pp. 1064–1069, 1995.

[24]M. L. da Silva, J. Loureiro, and V. Guerra, "A multiquantum dataset for vibrational excitation and dissociation in high-temperature O_2–O_2 collisions," *Chemical Physics Letters*, vol. 531, pp. 28–33, 2012.

[25]A. Varandas and A. Pais, "A realistic double many-body expansion (dmbe) potential energy surface for ground-state o3 from a multiproperty fit to ab initio calculations, and to experimental spectroscopic, inelastic scattering, and kinetic isotope thermal rate data," *Molecular Physics*, vol. 65, no. 4, pp. 843–860, 1988.